



## Removal of Acid Orange 7 from water by electrochemically generated Fenton's reagent

Ali Özcan<sup>a</sup>, Mehmet A. Oturan<sup>b,\*</sup>, Nihal Oturan<sup>b</sup>, Yücel Şahin<sup>a</sup>

<sup>a</sup> Anadolu University, Faculty of Science, Department of Chemistry, 26470 Eskişehir, Turkey

<sup>b</sup> Université Paris-Est, Laboratoire Géomatériaux et Géologie de l'Ingénieur, 5 bd Descartes, 77454 Marne-la-Vallée Cedex 2, France

### ARTICLE INFO

#### Article history:

Received 20 May 2008

Received in revised form 19 July 2008

Accepted 21 July 2008

Available online 26 July 2008

#### Keywords:

Advanced oxidation process

Electro-Fenton

Hydroxyl radicals

Acid Orange 7

Degradation

Mineralization pathway

### ABSTRACT

The removal of azo dye Acid Orange 7 (AO7) from water was investigated by the electro-Fenton technology using electrogenerated hydroxyl radicals ( $\cdot\text{OH}$ ) which leads to the oxidative degradation of AO7 up to its complete mineralization.  $\text{H}_2\text{O}_2$  and Fe (II) ions are electrogenerated in a catalytic way at the carbon-felt cathode. AO7 decay kinetics and evolution of its oxidation intermediates were monitored by high-performance liquid chromatography. The absolute rate constant of AO7 hydroxylation reaction has been determined as  $(1.20 \pm 0.17) \times 10^{10} \text{ M}^{-1} \text{ s}^{-1}$ . The optimal current value for the degradation of AO7 was found as 300 mA. AO7 degradation rate was found to decrease by increase in  $\text{Fe}^{3+}$  concentration beyond 0.1 mM. Mineralization of AO7 aqueous solutions was followed by total organic carbon (TOC) measurements and found to be 92%. Based on TOC evolution and identification of aromatic intermediates, short-chain carboxylic acids and inorganic ions released during treatment, a plausible mineralization pathway was proposed.

© 2008 Elsevier B.V. All rights reserved.

### 1. Introduction

Synthetic dyes are extensively used in textile, leather, paper, pharmaceutical and food industries. They thus constitute the major components of wastewaters released from these industries. The dyes are generally designed to resist biodegradation, so they cause severe ecological and environmental problems [1]. This environmental problem is highlighted by estimation of a charge up to 50,000 tons of dye wastes discharged annually from dyeing installations worldwide [2]. In addition, some dyes or their metabolites are either toxic or mutagenic and carcinogenic [3–4]. Thus, the treatment of the effluents containing such compounds is important for the protection of natural waters and environment.

Common physico-chemical treatment methods for the decolourization of dye wastewaters such as activated carbon adsorption and extraction are able to separate these pollutants to form a concentrated waste to be treated subsequently, and so they are inefficient to eliminate the pollutants. Ozone and hypochlorite oxidations are efficient decolourizing methods, but they are not desirable because of the high cost of equipment, operating costs and the secondary pollution arising from the

residual chlorine [5] or because of remained oxidation reaction intermediates. Other conventional processes based on biological treatment (aerobic–anaerobic) are relatively ineffective in effluent decolourization, because high molecular weight compounds are not easily degraded by bacteria, and thus coloured compounds pass through the treatment system largely undegraded [6].

Recent progress in the removal of dyes from water has led to the development of advanced oxidation processes (AOPs). These processes involve chemical, photochemical or electrochemical techniques to bring about chemical degradation of organic pollutants. The principal active species in such systems is the hydroxyl radical ( $\cdot\text{OH}$ ), a highly oxidizing agent of organic contaminants [7–10]. These radicals react with organic pollutants and thus lead to their degradation by three modes of action: hydrogen atom abstraction, electrophilic addition to  $\pi$  systems or electron transfer (redox) reactions.

The most commonly used AOPs for the removal of persistent organic pollutants from water are those based on the Fenton's reaction. Among the different Fenton-like technologies currently available, indirect electrochemical treatment has appeared to be quite efficient in eliminating organic pollutants from aqueous media [11–15]. This technology uses the Fenton's reaction as the source of hydroxyl radicals, in which the Fenton reagent, a mixture of  $\text{H}_2\text{O}_2$  and Fe (II), is produced electrochemically and regenerated throughout the process [16–18]. Because hydroxyl radicals production does not involve the use of harmful chemical reagents which

\* Corresponding author. Tel.: +33 149 32 90 65; fax: +33 149 32 91 37.

E-mail addresses: [aozcan3@anadolu.edu.tr](mailto:aozcan3@anadolu.edu.tr) (A. Özcan), [mehmet.oturan@univ-paris-est.fr](mailto:mehmet.oturan@univ-paris-est.fr) (M.A. Oturan).

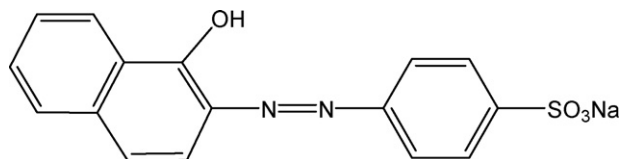
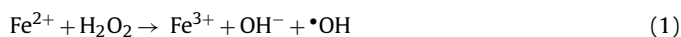


Fig. 1. The molecular structure of Acid Orange 7.

can be hazardous for the environment, this process is environmentally friendly for wastewater treatment and seems to be promising for the purification of water polluted by persistent and/or toxic organic pollutants [19–22].

The azo dye AO7, also called Orange II (Fig. 1) is a widely used synthetic dye. It does not decompose biologically, and resists to light irradiation and chemical oxidation. It is generally used as a model substrate for the aromatic azo dyes. Therefore, its degradation has been studied by several research groups; Bandara et al. [23] used photo-Fenton reactions in the presence of natural sunlight, Kiwi et al. [24] reported a catalytic photo-assisted system,  $\text{Fe}^{3+}$ /nafion/glass fibers, Daneshvar et al. [25] employed electrocoagulation, Ray et al. [26] performed photocatalytic oxidation in the presence of  $\text{TiO}_2$ , Ramirez et al. [27] investigated optimum conditions for Fenton's oxidation and Inoue et al. [28] used ultrasound waves. In addition, Daneshvar et al. [29] were studied the electrochemical degradation of Orange II in potentiostatic conditions and obtained a mineralization ratio of 75%.

In this study, we report a detailed discussion on the oxidative degradation of AO7 in acidic aqueous solution containing catalytic amount of  $\text{Fe}^{3+}$  by using an indirect electrochemical method, the electro-Fenton process. The experiments were carried out under constant current electrolysis conditions in an undivided electrochemical cell by using a carbon-felt cathode and a Pt anode. The process involves electrochemically assisted Fenton's reaction (reaction (1)) in which  $\text{H}_2\text{O}_2$  and  $\text{Fe}^{2+}$  ions are electrogenerated in a catalytic way [30–33]:



The kinetics of AO7 degradation by  $\bullet\text{OH}$  during electro-Fenton process has been examined. The absolute rate constant of the reaction between AO7 and  $\bullet\text{OH}$  was determined by the competition kinetic method [34–35] using benzoic acid as a reference competitor. The effect of the applied current and catalyst concentration on the degradation of AO7 was studied. The main oxidative degradation reaction intermediates were identified by using several chromatographic techniques. Finally a mineralization reaction pathway for the degradation of AO7 by electrochemically generated  $\bullet\text{OH}$  was proposed from the basis of identified aromatic oxidation intermediates, aliphatic short-chain carboxylic acids as end-products before mineralization and inorganic ions released to the solution.

## 2. Materials and methods

### 2.1. Materials

AO7 (Tropaeolin 000 no. 2; Orange II, Fig. 1) was obtained from Fluka. Iron (III) sulphate pentahydrate (97%, Across), iron (III) chloride (98%, Labosi), sodium sulphate (anhydrous, 99%, Across), benzoic acid, sulphuric acid, salicylic acid (ACS reagent grade, Across) sodium carbonate (ACS reagent grade, Riedel-de Haën), sodium bicarbonate (99.7%, Fluka), acetic acid (glacial p.a., Across) and potassium hydrogen phthalate (Nacalai tesque Inc.) were obtained as reagent grade and used without further purification.

All solutions were prepared by using pre-distilled  $18 \mu\text{S cm}^{-1}$  deionized water (Sartorius).

### 2.2. Electrochemical cell and equipment

Experiments were performed at room temperature in a 0.25-L undivided cylindrical glass cell of diameter of 6 cm equipped with two electrodes. The working electrode was a  $60 \text{ cm}^2$  piece of carbon-felt ( $17 \text{ cm} \times 3.5 \text{ cm}$ ). It is placed on the inner wall of the cell covering the totality of the internal perimeter. The counter electrode was cylindrical Pt gauze placed on the centre of the cell. Prior to the electrolysis, compressed air was bubbled through the aqueous solutions, which were agitated continuously by a magnetic stirrer at 500 rpm. A catalytic quantity of ferrous ion was introduced into the solution before the beginning of electrolysis. The applied current was 60, 100 and 300 mA for degradation kinetic, by-products identification and mineralization experiments, respectively. The current and the amount of charge passed through the solution were measured and displayed continuously throughout electrolysis by using a DC power supply. The initial pH of solutions was set to 3 by addition of aqueous  $\text{H}_2\text{SO}_4$  (1 M) and HCl (1 M). The pH values were measured by a pH glass electrode calibrated with standard buffers at pH values of 4 and 7. It remains between 3.0 and 2.8 during electrolyses;  $\text{H}^+$  consumed by cathodic reactions being compensated by water oxidation at the anode. The ionic strength was maintained constant (50 mM) by addition of  $\text{Na}_2\text{SO}_4$ .

### 2.3. High-performance liquid chromatography (HPLC)

The degradation of AO7 was monitored by high-performance liquid chromatography (HPLC) using a Merck Lachrom system equipped with an L-7455 diode array detector and fitted with a reverse phase Purospher RP-18, 5- $\mu\text{m}$ , 4.6 mm  $\times$  250 mm column from Merck. The column was placed in an oven (Merck L-7350) which was thermostated at  $40^\circ\text{C}$ . Injection volumes were 20  $\mu\text{L}$ . The column was eluted at isocratic mode with a mixture of water–methanol–acetic acid 19:79:2 (v/v) with a flow rate of  $1.1 \text{ mL min}^{-1}$ . Detection was performed at 486 nm. Short-chain carboxylic acids were identified and quantified using the above HPLC system by a Supelcogel H column ( $\phi = 7.8 \text{ mm} \times 300 \text{ mm}$ ) with a mobile phase of 4 mM  $\text{H}_2\text{SO}_4$ . The detection was performed at 210 nm. Calibration curves were obtained by using the pure standards of the related carboxylic acids.

### 2.4. Gas chromatography–mass spectrometry (GC–MS)

In order to identify the AO7 aromatic degradation products, GC–MS analyses were performed. After electrolysis, the aqueous solutions were filtered and extracted three times with dichloromethane and ethylacetate. After that, these solutions were concentrated by evaporation of the solvent to a volume of about 2 mL. The final solution was analysed in a GC–MS instrument (Finnigan PolarisQ), equipped with a 30 m SE54 fused silica capillary column. A gradient temperature program at  $10^\circ\text{C min}^{-1}$  was applied between 40 and  $280^\circ\text{C}$ .

### 2.5. Ion chromatography (IC)

The concentration of ammonium, nitrate and sulphate ions released during electrolysis was measured by ion chromatography (Dionex ICS-1000 equipped with a conductivity detector). A cationic exchanger column (IonPac<sup>®</sup> CS12A-Dionex) was used for ammonium ion and an anionic exchanger column (IonPac<sup>®</sup> AS14-Dionex) was used for nitrate and sulphate ions. The volume of injections was 10  $\mu\text{L}$ . The mobile phase was 11.0 mM sulphuric acid

with a flow rate of  $1.0 \text{ mL min}^{-1}$  for the cationic column and a mixture of  $1.8 \text{ mM}$  sodium carbonate and  $1.7 \text{ mM}$  sodium hydrogen carbonate solution with a flow rate of  $2.0 \text{ mL min}^{-1}$  for the anionic column. Calibration curves were obtained by using the pure standards of the related ions.

### 2.6. Total organic carbon (TOC) analysis

The TOC of the initial and treated samples was determined by a Shimadzu 5000 TOC-V<sub>CSH</sub> analyser.

Samples of  $50 \mu\text{L}$  were acidified with  $\text{H}_2\text{SO}_4$  before injection in order to obtain pH 2 and avoid mineral carbon (carbonate or bicarbonate ions) in solution. TOC measurements were based on the combustion of organics and detection of  $\text{CO}_2$  formed by infrared gas analysis method. Calibration of the analyser was achieved with potassium hydrogen phthalate standards.

## 3. Results and discussion

### 3.1. Indirect electrochemical hydroxyl radicals production

Hydroxyl radicals were in situ generated via Fenton's reaction Eq. (1) assisted by electrochemistry. In optimal process conditions (pH 3) the predominant species of iron (III) is  $\text{Fe}(\text{OH})^{2+}$ . Consequently, the Fenton's reaction can be read as follows:



This reaction can be propagated in a catalytic way from  $\text{Fe}^{2+}$  regeneration, which mainly takes place by reduction of  $\text{Fe}^{3+}$  species at the cathode surface, thus avoiding the production of iron sludge [9,36]:



On the other hand  $\text{H}_2\text{O}_2$  is continuously produced in solution from the two-electron reduction of dissolved  $\text{O}_2$  [13,17]:



The anodic reaction consists of the oxidation of water at Pt electrode, thus supplying oxygen to Eq. (4):



The sum of the above cathodic and anodic equations gives the following overall equation [11]:



This last reaction shows well the catalytic character of the electro-Fenton process in which two moles of hydroxyl radical were generated in a catalytic way without intervention of chemical reagents.

### 3.2. The effect of the applied current on the degradation kinetics

Oxidation of AO7 in acidic aqueous medium with electrochemically generated hydroxyl radicals was performed at current-controlled conditions at room temperature. The disappearance of AO7 was followed by HPLC analysis during electrolysis. In the electro-Fenton process the applied current is an important parameter for the operational cost and process efficiency. The effect of applied current on the decay kinetics of AO7 was investigated by conducting constant current electrolysis at different current values, i.e., 30, 60, 100, 300, and 500 mA. It can be seen from Fig. 2 that the concentration of AO7 decreases exponentially for all current values. The increasing of the applied current enhances rate of the  $\text{H}_2\text{O}_2$

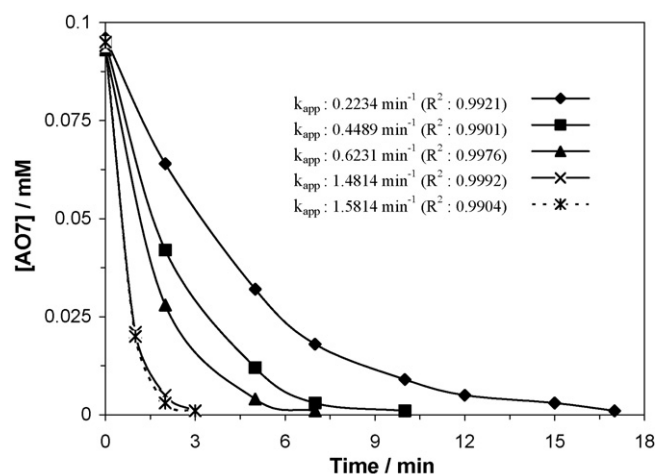


Fig. 2. Degradation kinetics of AO7 in acidic media at several current values by electro-Fenton process— $I$ : 30 mA ( $\blacklozenge$ ); 60 mA ( $\blacksquare$ ); 100 mA ( $\blacktriangle$ ); 300 mA ( $\times$ ); 500 mA ( $\ast$ ).  $C_0$ : 0.10 mM;  $[\text{Fe}^{3+}]$ : 0.2 mM;  $[\text{Na}_2\text{SO}_4]$ : 50 mM;  $V$ : 0.200 L; pH: 3.

electrogeneration (Eq. (3)) and consequently those of  $\bullet\text{OH}$  production Eq. (2). The oxidation of water on the anode surface may form hydroxyl radicals Eq. (7). These radicals lead to anodic oxidation of organics. Therefore, to evaluate the influence of anodic oxidation on the degradation of AO7, experiments were performed in the  $\text{Fe}^{3+}$  free solution at 300 mA (Fig. 3). A graphite bar was used as cathode instead of carbon felt to prevent the formation of hydrogen peroxide during the electrolysis. As can be seen from Fig. 3, only 4.1% of 0.1 mM AO7 degraded in 3 min treatment by the anodic oxidation process. On the other hand, the complete degradation of 0.1 mM AO7 was achieved in 3 min at the same conditions in the case of electro-Fenton process. This situation can be explained in the following way, the formed hydroxyl radicals are tightly adsorbed to the Pt anode surface; therefore, their oxidation abilities are very limited. This situation was reported in the literature many times [12,20]. Because of these reasons, we did not take into account the contribution of anodic oxidation in the rest of the study.



The exponential decrease of AO7 concentration during the electro-Fenton treatment indicates a pseudo first order reaction kinetics for oxidation of AO7 by  $\bullet\text{OH}$ . Considering the steady state

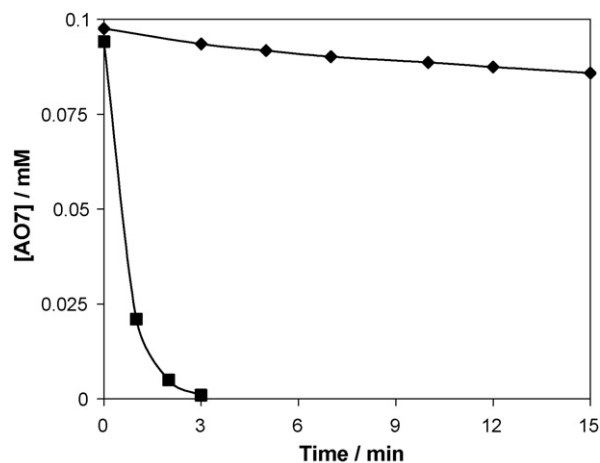


Fig. 3. Degradation kinetics of 0.1 mM AO7 in acidic media by the anodic oxidation with Pt anode ( $\blacklozenge$ ) and electro-Fenton\* ( $\blacksquare$ ) process.  $I$ : 300 mA;  $[\text{Na}_2\text{SO}_4]$ : 50 mM;  $V$ : 0.200 L; pH: 3.  $[\text{Fe}^{3+}]$ : 0.2 mM.

approximation for  $\bullet\text{OH}$ , the AO7 oxidation rate expression can be written:

$$-\frac{d[\text{AO7}]}{dt} = k_{\text{AO7}} [\bullet\text{OH}] [\text{AO7}] = k_{\text{app}(\text{AO7})} [\text{AO7}] \quad (8)$$

Apparent rate constants for the degradation of AO7 were determined by plotting the  $\text{Ln}([\text{AO7}]_0/[\text{AO7}])$  against time at different current values (inset of Fig. 2). The values of 0.22, 0.45, 0.62, 1.48 and  $1.58 \text{ min}^{-1}$  were obtained for 30, 60, 100, 300, and 500 mA, respectively. When the applied current value was increased from 30 to 60 mA, the apparent rate constant value increased twofold. There was a gradual rise in the apparent rate constant values between 60 and 300 mA. However, the apparent rate constant did not increase linearly with the current. After approximately 300 mA, the apparent rate constant reached a steady state and remained almost constant. These results shows that the rate of  $\text{H}_2\text{O}_2$  electrogeneration is limited by mass transfer for  $I > 300 \text{ mA}$ . Fig. 2 shows that at  $I = 300 \text{ mA}$ , the total disappearance of AO7 in a solution of 0.10 mM require only 3 min. Consequently, the value of 300 mA was selected for the mineralization experiments.

The absolute rate constant  $k_{\text{abs}}$  for AO7 hydroxylation reaction can be determined then using the competition kinetic method [34–35]. Benzoic acid was selected as standard competitor because the  $k_{\text{abs}}$  of its hydroxylation reaction is well known ( $k_{\text{BA}} = 4.3 \times 10^9 \text{ M}^{-1} \text{ s}^{-1}$ ). AO7 and BA were introduced in the solution at same initial concentration.

$$-\frac{d[\text{BA}]}{dt} = k_{\text{BA}} [\bullet\text{OH}] [\text{BA}] = k_{\text{app}(\text{BA})} [\text{BA}] \quad (9)$$

The ratio of integrated form of Eqs. (8) and (9) allows determining the  $k_{\text{AO7}}$  according to the following equation:

$$k_{\text{AO7}} = k_{\text{BA}} \left\{ \frac{\text{Ln} \left( \frac{[\text{AO7}]_0}{[\text{AO7}]_t} \right)}{\text{Ln} \left( \frac{[\text{BA}]_0}{[\text{BA}]_t} \right)} \right\} \quad (10)$$

The absolute rate constant  $k_{\text{AO7}}$  of the reaction between AO7 and  $\bullet\text{OH}$  was calculated from Eq. (10) as  $(1.20 \pm 0.17) \times 10^{10} \text{ M}^{-1} \text{ s}^{-1}$ . Lopez and Kiwi [37] reported the value of  $6.0 \times 10^9 \text{ M}^{-1} \text{ s}^{-1}$  for AO7 hydroxylation reaction by using a membrane based reactor system. The greater rate constant value determined in this study is in agreement with the quick AO7 destruction rate observed in Fig. 2.

### 3.3. Effect of $\text{Fe}^{3+}$ (catalyst) concentration on the AO7 oxidation and mineralization efficiency

The initial oxidation kinetic of AO7 by  $\bullet\text{OH}$  generated during electro-Fenton process and the mineralization efficiency of AO7 containing aqueous solutions were investigated by using 0.1 mM AO7 in the presence of different  $\text{Fe}^{3+}$  concentrations in acidic media of pH 3. The applied current values for the degradation and mineralization experiments were 60 and 300 mA, respectively. The effect of the  $\text{Fe}^{3+}$  concentration on the degradation of AO7 was shown in Fig. 4. As can be seen from this figure that the degradation rate increases with increasing  $\text{Fe}^{3+}$  concentration from 0.05 to 0.10 mM. After this value, the degradation rate decreases by increasing  $\text{Fe}^{3+}$  concentration.

Fig. 5 shows the influence of catalyst ( $\text{Fe}^{3+}$ ) concentration on the mineralization of AO7 aqueous solutions in term of TOC removal. The TOC removal was almost 60% in the first hour of electrolysis in the presence of 0.1 mM  $\text{Fe}^{3+}$ . In the case of 0.2, 0.5, and 1.0 mM  $\text{Fe}^{3+}$ , TOC removal values were 48, 36, and 26%, respectively. TOC removal values were reached 92 and 56% after 8 h electro-Fenton treatment for the 0.1 and 1.0 mM  $\text{Fe}^{3+}$  concentrations, respectively.

The negative influence of the higher catalyst concentration on degradation kinetics and mineralization can be explained by the increase of the rate of parasitic reactions Eqs. (11)–(13) occurred

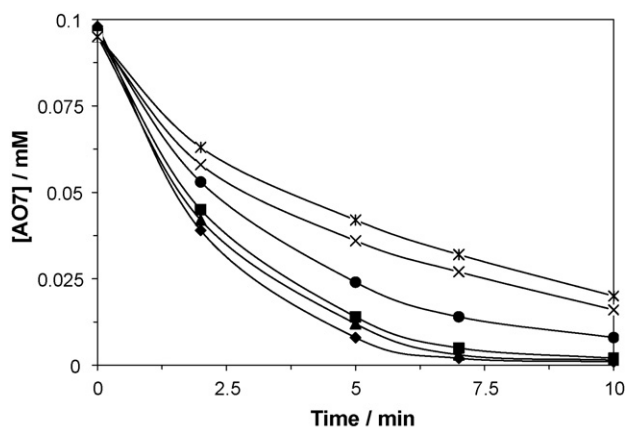
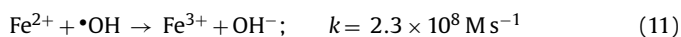


Fig. 4. Degradation kinetics of AO7 in acidic media at several catalyst concentration by electro-Fenton process— $[\text{Fe}^{3+}]$ : 0.05 mM (■); 0.10 mM (◆); 0.20 mM (▲); 0.50 mM (●); 1.00 mM (×); 2.00 mM (✱).  $C_0$ : 0.1 mM;  $[\text{Na}_2\text{SO}_4]$ : 50 mM;  $I$ : 60 mA;  $V$ : 0.200 L; pH: 3.

during the process between hydroxyl radicals and iron species:



When the  $\text{Fe}^{3+}$  concentration increased in the medium, the percentage of the scavenged hydroxyl radicals increased following the waste reaction (11) [38]. Moreover,  $\text{Fe}^{3+}$  ion could react with  $\text{H}_2\text{O}_2$  to form hydroperoxyl radicals Eqs. (12) and (13) [39] which is significantly less oxidizing agent than  $\bullet\text{OH}$ .

### 3.4. Analysis of aromatic degradation products of AO7

In order to identify the aromatic oxidation products of AO7, an aqueous solution of 1.0 mM was electrolysed 100 mA by using at the conditions of the degradation experiments. Identification of formed aromatic oxidation reaction intermediates were performed by using HPLC and GC–MS analyses. The HPLC identification was

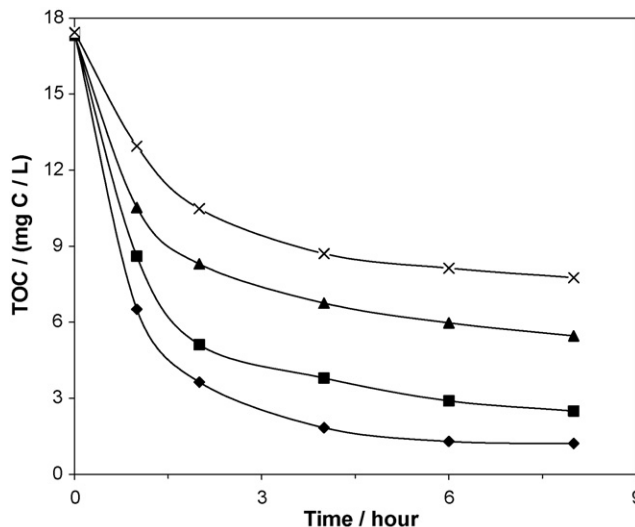


Fig. 5. TOC values during the mineralization of AO7 in acidic media at several catalyst concentration by electro-Fenton process— $[\text{Fe}^{3+}]$ : 0.10 mM (◆); 0.20 mM (■); 0.50 mM (▲); 1.00 mM (×).  $C_0$ : 0.1 mM;  $[\text{Na}_2\text{SO}_4]$ : 50 mM;  $I$ : 300 mA;  $V$ : 0.225 L; pH: 3.



carried out by comparison of the retention time and using the standard addition method. On the other hand, the GC–MS identification of products was performed by comparing the obtained spectrums with the spectrums of standard compounds obtained in the same way. The identified aromatic intermediates obtained at our experimental conditions were shown in Table 1. Compounds I, II, III, IV, VI, and VIII were identified by HPLC analysis. Compounds IX, X, XI and XII were determined by GC–MS analysis, whereas compounds V and VII were identified by both HPLC and GC–MS analyses. Some of the determined intermediates such as VI [23,40–41] and VII [23,41], II, IX and XI [29] has been already reported by using different AOPs ranging from ozonation to biodegradation or electrooxidation.

### 3.5. Identification and evolution of short-chain carboxylic acids

Electro-Fenton treated solutions were analysed in order to identify and quantify the short-chain carboxylic acids formed by the oxidative ring opening reactions of polyhydroxylated or quinones derivatives. Oxalic, maleic, glyoxylic, malonic, formic and acetic acid were detected at 8.70, 9.87, 11.92, 13.13, 16.05 and 17.61 min of retention time, respectively, under our analysis conditions. Fig. 6a shows their evolution as function of electrolysis time during electro-Fenton treatment of a 0.1 mM AO7 aqueous solution of pH 3. These acids are generated as soon as the electrolysis started with a large formation rate for oxalic, glyoxylic, malonic, acetic, and formic acids. The curves corresponding to evolution of glyoxylic and acetic acids (Fig. 6a) show their disappearance to the profit of formic and oxalic acids which are usually final by-products before complete mineralization during treatments by advanced oxidation techniques [12,13,42,43]. Vel Leitner and Doré [44] showed that the oxalic acid was the main by-product of the oxidation of glyoxylic acid. On the other hand, the oxidation of acetic acid to oxalic acid was also reported [45]. Concerning the maleic acid, it is present throughout electrolysis but in a very low concentration.

### 3.6. Identification and evolution of inorganic ions

The ion chromatography analysis allowed qualitative and quantitative monitoring of inorganic ions resulting from the electro-Fenton treatment of 0.10 mM AO7 aqueous solution. Evolution of released  $\text{NO}_3^-$ ,  $\text{SO}_4^{2-}$  and  $\text{NH}_4^+$  ions concentration during electrolysis is presented in Fig. 6b. The concentration of  $\text{SO}_4^{2-}$  ions formed from AO7 mineralization reached the value of 0.0515 mM in the first hour of electrolysis. This indicates that the most of ( $-\text{SO}_3^-$ ) group present in AO7 structure was oxidized at the early stage of the treatment.  $\text{SO}_4^{2-}$  concentration reached 0.094 mM at the end of the electrolysis. The cleavage of the  $-\text{N}=\text{N}-$  bond of AO7 led to the

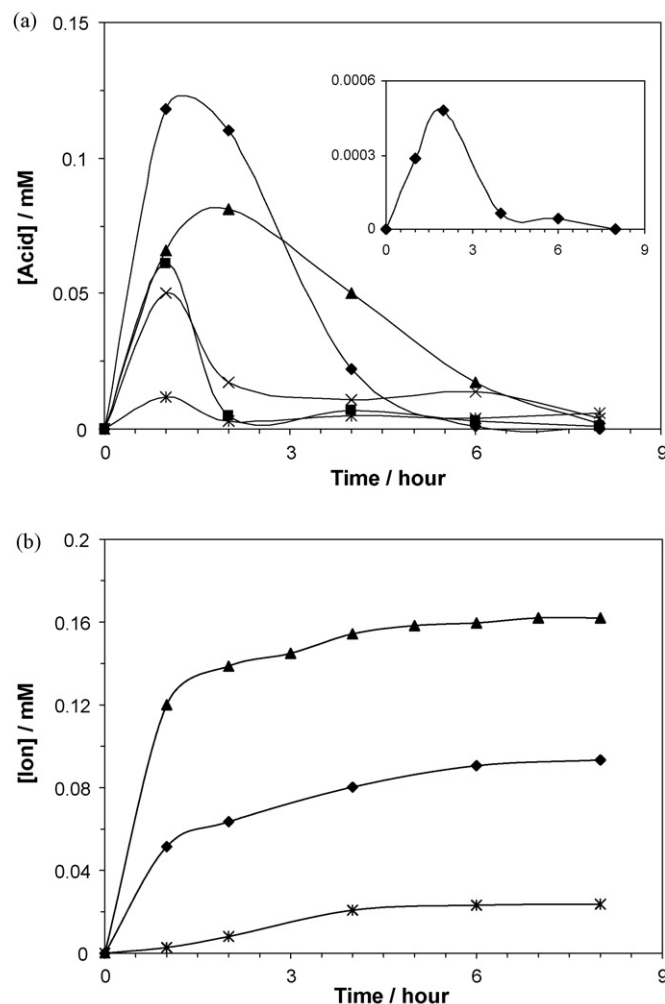


**Fig. 6.** Time-course of carboxylic acids (a) and inorganic ions (b) concentration during electro-Fenton treatment of an aqueous solution of AO7 in HCl medium.  $C_0$ : 0.10 mM;  $[\text{Fe}^{3+}]$ : 0.1 mM;  $I$ : 100 mA;  $V$ : 0.225 L; pH: 3. (a) Oxalic acid ( $\blacklozenge$ ), glyoxylic acid ( $\blacksquare$ ), malonic acid ( $\blacktriangle$ ), formic acid ( $\times$ ) and acetic acid ( $\times$ ). Inset: maleic acid ( $\blacklozenge$ ). (b) Nitrate ( $\times$ ); sulphate ( $\blacklozenge$ ); ammonium ( $\blacktriangle$ ).

formation of the intermediates containing ( $-\text{NO}_2$ ) [46] and ( $-\text{NH}_2$ ) [23] substituents. These groups were oxidized to nitrate and ammonium ions, respectively, during the mineralization of corresponding intermediates by of hydroxyl radicals. The results showed that the nitrogen initially presented in AO7 was converted predominantly

**Table 1**

HPLC retention time ( $t_R$ ) and GC/MS spectra of aromatic by-products formed during the electro-Fenton treatment of AO7

No	Compound name	HPLC	GC/MS	Mass fragmentation
		$t_R$ /min	$t_R$ /min	
I	4-Aminophenol	3.40	–	
II	4-Aminobenzenesulphonic acid	3.75	–	
III	1,2,4-Benzenetriol	5.40	–	
IV	Hydroquinone	8.0	–	
V	1,4-Benzoquinone	14.75	5.59	108 ( $M^+$ ), 82, 54
VI	4-Hydroxybenzenesulphonic acid	20.06	–	
VII	1,2-Naphthaquinone	24.75	15.40	158 ( $M^+$ ), 130, 102, 76
VIII	Salicylic acid	29.20	–	
IX	2-Formyl-benzoic acid	–	14.00	149 ( $M^+$ ), 122, 105, 77, 51
X	2-Hydroxy-1,4-naphthalenedione	–	14.57	174 ( $M^+$ ), 146, 118, 105, 77
XI	1,2-Naphthalenediol	–	15.94	160 ( $M^+$ ), 131, 114, 103, 77
XII	2,3-Dihydroxy-1,4-naphthalenedione	–	16.84	190 ( $M^+$ ), 162, 131, 105, 88, 77

Experimental conditions:  $C_0 = 1.0$  mM;  $[\text{Fe}^{3+}] = 0.1$  mM;  $[\text{Na}_2\text{SO}_4] = 50$  mM; pH 3;  $I = 100$  mA.



to  $\text{NH}_4^+$  ions. After 8 h of electrolysis, the sum of  $\text{NO}_3^-$  and  $\text{NH}_4^+$  ions concentrations was reached almost 98% of initial nitrogen of AO7 indicating its overall mineralization.

### 3.7. Degradation pathway of AO7 mineralization

Data obtained on the oxidation kinetic of AO7, identification and evolution of its aromatic reaction intermediates, aliphatic short-chain carboxylic acids and released inorganic ions as well as evolution of TOC abatement during electro-Fenton treatment allow us to propose a schematic degradation pathway of AO7 by electrochemically generated hydroxyl radicals (Fig. 7). The oxidative degradation of AO7 starts with the breaking of the azo bond, the most active group in the structure [23], to form compound II and XI. The oxidation of AO7 leading until mineralization occurs then in three stages. In the first one, the oxidative cleavage of AO7 leads to the formation of II and XI. The second stage includes the hydroxylation of these intermediates to hydroxylated (I and VI) or polyhydroxylated (III and IV) derivatives which are oxidized in their turn to the quinoid (V, VII, VIII, IX and XII) structures. Formation of X and XII is supposed from 1,2,4-trihydroxynaphthalene which is not detected in our experimental conditions. Polyhydroxylated and quinoid structures are unstable and leads to the formation of short-chain carboxylic acids by oxidative ring opening reactions. Oxidation of the formed carboxylic acids to  $\text{CO}_2$ , the final oxidation stage of organics, constitutes the last stage of mineralization.

## 4. Conclusions

Electrochemically generated Fenton's reagent was used to produce  $\bullet\text{OH}$  to eliminate the azo dye AO7 from aqueous medium. We showed that the degradation kinetics and mineralization efficiency were increased by increasing the applied current and decreasing the concentration of  $\text{Fe}^{3+}$  ions as catalyst. At the optimal experimental conditions ( $I = 300 \text{ mA}$ ,  $[\text{Fe}^{3+}] = 0.1 \text{ mM}$  and  $\text{pH} 3$ ), the complete disappearance of AO7 in aqueous medium required only 3 min. The absolute rate constant of the reaction between AO7 and  $\bullet\text{OH}$  was determined as  $k_{\text{AO7}} = (1.2 \pm 0.17) \times 10^{10} \text{ M}^{-1} \text{ s}^{-1}$ . Complete destruction of AO7 and its aromatic by-products was achieved in less than 1 h. The quasi complete mineralization of a 0.10 mM AO7 aqueous solution was achieved in 8 h.

Oxidative degradation of AO7 during electro-Fenton treatment leads to the formation of aromatic reaction intermediates. Several aromatic intermediates such as 1,2-naphthaquinone, 1,2-naphthalenediol, 4-aminobenzenesulphonic acid, 4-aminophenol, 4-hydroxybenzenesulphonic acid, 2-formyl-benzoic acid, 2-hydroxy-1,4-naphthalenedione, 2,3-dihydroxy-1,4-naphthalenedione, salicylic acid, 1,4-benzoquinone, hydroquinone and 1,2,4-benzotriazol as well as the some short-chain carboxylic acids (maleic, acetic, malonic, glyoxylic, formic and oxalic) and inorganic ions ( $\text{SO}_4^{2-}$ ,  $\text{NO}_3^-$  and  $\text{NH}_4^+$ ) were identified using HPLC, IC and GC-MS analyses. This information permitted to propose a plausible mineralization reaction pathway of AO7.

Electro Fenton process seems to be an economically and environmentally friendly process to remove the toxicity of the persistent organic pollutants from water. The main oxidizing species,  $\bullet\text{OH}$ , being a non-selective oxidizing reagent, the process can be generalized to other organic pollutants.

## Acknowledgements

This work was supported by Anadolu University Research Found (Project no: 061022). Ali Özcan express his gratitude to The Scien-

tific and Technical Research Council of Turkey (TUBITAK) Scientific Human Resources Development (BAYG) for the fellowship.

## References

- [1] S.J. Allen, K.Y.H. Khader, M. Bino, Electrooxidation of dyestuffs in waste waters, *J. Chem. Tech. Biotechnol.* 62 (1) (1995) 111–117.
- [2] D. Brown, Effects of colorants in the aquatic environment, *Chemosphere* 12 (3) (1987) 397–404.
- [3] G.S. Heiss, B. Gowan, E.R. Dabbs, Cloning of DNA from a Rhodococcus strain conferring the ability to decolorize sulfonated azo dyes, *FEMS Microbiol. Lett.* 99 (2/3) (1992) 221–226.
- [4] K.C. Chen, J.Y. Wu, C.C. Huang, Y.M. Liang, S.C.J. Hwang, Decolorization of azo dye using PVA-immobilized microorganisms, *J. Biotechnol.* 101 (3) (2003) 241–252.
- [5] P.K. Malik, S.K. Saha, Oxidation of direct dyes with hydrogen peroxide using ferrous ion as catalyst, *Sep. Purif. Technol.* 31 (3) (2003) 241–250.
- [6] I.M. Banat, P. Nigam, D. Singh, R. Marchant, Microbial decolourisation of textile-dye-containing effluents: a review, *Biores. Technol.* 58 (3) (1996) 217–227.
- [7] S.H. Lin, C.C. Lo, Fenton process for treatment of desizing wastewater, *Water Res.* 31 (8) (1997) 2050–2056.
- [8] P.L. Huston, J.J. Pignatello, Degradation of selected pesticide active ingredients and commercial formulations in water by the photo-assisted Fenton reaction, *Water Res.* 33 (5) (1999) 1238–1246.
- [9] M.A. Oturan, An ecologically effective water treatment technique using electrochemically generated hydroxyl radicals for in situ destruction of organic pollutants, *J. Appl. Electrochem.* 30 (4) (2000) 475–482.
- [10] K. Dutta, S. Mukhopadhyay, S. Bhattacharjee, B. Chaudhuri, Chemical oxidation of methylene blue using a Fenton-like reaction, *J. Hazard. Mater.* B84 (2001) 57–71.
- [11] M.A. Oturan, N. Oturan, C. Lahite, S. Trévin, Production of hydroxyl radicals by electrochemically assisted Fenton's reagent. Application to the mineralization of an organic micropollutant, pentachlorophenol, *J. Electroanal. Chem.* 507 (1/2) (2001) 96–102.
- [12] B. Boye, M.M. Dieng, E. Brillas, Anodic oxidation, electro-Fenton and photoelectro-Fenton treatments of 2,4,5-trichlorophenoxyacetic acid, *J. Electroanal. Chem.* 557 (1) (2003) 135–146.
- [13] E. Brillas, E. Mur, R. Saucedo, L. Sanchez, J. Peral, X. Domenech, Aniline mineralization by AOPs: anodic oxidation, photocatalysis, electro-Fenton and photo-Fenton processes, *Appl. Catal. A: Environ.* 16 (1) (1998) 31–42.
- [14] N. Oturan, M.A. Oturan, Degradation of three pesticides used in viticulture by electrogenerated Fenton's reagent, *Agron. Sustain. Dev.* 25 (2) (2005) 267–270.
- [15] C. Flox, A. Ammar, C. Arias, E. Brillas, A.D. Vargas-Zavala, R. Abdelhedi, Electro-Fenton and photoelectro-Fenton degradation of indigo carmine in acidic aqueous medium, *Appl. Catal. B: Environ.* 67 (1/2) (2006) 93–104.
- [16] M.A. Oturan, J. Pinson, D. Deprez, B. Terlain, Polyhydroxylation of salicylic acid by electrochemically generated  $\bullet\text{OH}$  radicals, *New J. Chem.* 16 (1992) 705–710.
- [17] M.A. Oturan, J. Pinson, Hydroxylation by electrochemically generated OH radicals. Mono- and polyhydroxylation of benzoic acid: products and isomers' distribution, *J. Phys. Chem.* 99 (38) (1995) 13948–13954.
- [18] E. Brillas, M. Banos, J. Garrido, Mineralization of herbicide 3,6-dichloro-2-methoxybenzoic acid in aqueous media by anodic oxidation, electro-Fenton and photoelectro-Fenton, *Electrochim. Acta* 48 (12) (2003) 1697–1705.
- [19] B. Gözmen, M.A. Oturan, N. Oturan, O. Erbatır, Indirect electrochemical treatment of bisphenol A in water via electrochemically generated Fenton's reagent, *Environ. Sci. Technol.* 37 (16) (2003) 3716–3723.
- [20] E. Brillas, I. Sirés, C. Arias, P.L. Cabot, F. Centellas, R.M. Rodriguez, J.A. Garrido, Mineralization of paracetamol in aqueous medium by anodic oxidation with a boron-doped diamond electrode, *Chemosphere* 58 (4) (2005) 399–406.
- [21] I. Sirés, J.A. Garrido, R.M. Rodriguez, E. Brillas, N. Oturan, M.A. Oturan, Catalytic behavior of the  $\text{Fe}^{3+}/\text{Fe}^{2+}$  system in the electro-Fenton degradation of the antimicrobial chlorophene, *Appl. Catal. B: Environ.* 72 (3/4) (2007) 382–394.
- [22] A. Özcan, Y. Şahin, A.S. Kopalal, M.A. Oturan, Degradation of picloram by the electro-Fenton process, *J. Hazard. Mater.* 153 (1/2) (2008) 718–727.
- [23] J. Bandara, C. Morrison, J. Kiwi, C. Pulgarin, P. Peringer, Degradation/decoloration of concentrated solutions of orange II. Kinetics and quantum yield for sunlight induced reactions via Fenton type reagents, *J. Photochem. Photobiol. A: Chem.* 99 (1) (1996) 57–66.
- [24] J. Kiwi, M.R. Dhananjayan, J. Albers, O. Enea, Photo-assisted immobilized Fenton degradation up to pH 8 of azo dye orange II mediated by  $\text{Fe}^{3+}$ /nafion/glass fibers, *Helv. Chim. Acta* 84 (11) (2001) 3433–3445.
- [25] N. Daneshvar, H. Ashassi-Sorkhabi, A. Tizpar, Decolorization of orange II by electrocoagulation method, *Sep. Purif. Technol.* 31 (2) (2003) 153–162.
- [26] M.B. Ray, A. Bhattacharya, S. Kawi, Photocatalytic degradation of orange II by  $\text{TiO}_2$  catalysts supported on adsorbents, *Catal. Today* 98 (3) (2004) 431–439.
- [27] J.H. Ramirez, C.A. Costa, L.M. Madeira, Experimental design to optimize the degradation of the synthetic dye Orange II using Fenton's reagent, *Catal. Today* 107/108 (2005) 68–76.
- [28] M. Inoue, F. Okada, A. Sakurai, M. Sakakibara, A new development of dyestuffs degradation system using ultrasound, *Ultrason. Sonochem.* 13 (4) (2006) 313–320.
- [29] N. Daneshvar, S. Aber, V. Vatanpour, M.H. Rasoulifard, Electro-Fenton treatment of dye solution containing Orange II. Influence of operational parameters, *J. Electroanal. Chem.* 615 (2) (2008) 165–174.

- [30] M.A. Oturan, J. Pinson, J. Bizot, D. Deprez, B. Terlain, Reaction of inflammation inhibitors with chemically and electrochemically generated hydroxyl radicals, *J. Electroanal. Chem.* 334 (1/2) (1992) 103–109.
- [31] E. Brillas, B. Boye, I. Sirés, J.A. Garrido, R.M. Rodríguez, C. Arias, P.L. Cabot, C. Comninellis, Electrochemical destruction of chlorophenoxy herbicides by anodic oxidation and electro-Fenton using a boron-doped diamond electrode, *Electrochim. Acta* 49 (25) (2004) 4487–4496.
- [32] S. Hammami, N. Oturan, N. Bellakhal, M. Dachraoui, M.A. Oturan, Oxidative degradation of direct orange 61 by electro-Fenton process using a carbon felt electrode: application of the experimental design methodology, *J. Electroanal. Chem.* 660 (1) (2007) 75–84.
- [33] A. Özcan, Y. Şahin, A.S. Koparal, M.A. Oturan, Carbon sponge as a new cathode material for the electro-Fenton process. Comparison with carbon felt cathode and application to degradation of synthetic dye basic blue 3 in aqueous medium, *J. Electroanal. Chem.* 616 (1) (2008) 71–78.
- [34] M. Diagne, N. Oturan, M.A. Oturan, Removal of methyl parathion from water by electrochemically generated Fenton's reagent, *Chemosphere* 66 (5) (2007) 841–848.
- [35] K. Hanna, S. Chiron, M.A. Oturan, Coupling enhanced water solubilization with cyclodextrin to indirect electrochemical treatment for pentachlorophenol contaminated soil remediation, *Water Res.* 39 (12) (2005) 2763–2773.
- [36] B. Boye, M.M. Dieng, E. Brillas, Degradation of herbicide 4-chlorophenoxyacetic acid by advanced electrochemical oxidation methods, *Environ. Sci. Technol.* 36 (13) (2002) 3030–3035.
- [37] A. Lopez, J. Kiwi, Modeling the performance of an innovative membrane-based reactor. Abatement of azo dye (Orange II) up to biocompatibility, *Ind. Eng. Chem. Res.* 40 (8) (2001) 1852–1858.
- [38] F.J. Benitez, J.L. Acero, F.J. Real, F.J. Rubio, A.I. Leal, The role of hydroxyl radicals for the decomposition of *p*-hydroxy phenylacetic acid in aqueous solutions, *Water Res.* 35 (5) (2001) 1338–1343.
- [39] E. Neyens, J. Baeyens, A review of classic Fenton's peroxidation as an advanced oxidation technique, *J. Hazard. Mater.* 98 (1–3) (2003) 33–50.
- [40] K. Hustert, R.G. Zepp, Photocatalytic degradation of selected azo dyes, *Chemosphere* 24 (3) (1992) 335–342.
- [41] J.T. Spadaro, L. Isabelle, V. Ranganathan, Hydroxyl radical mediated degradation of azo dyes: evidence for benzene generation, *Environ. Sci. Technol.* 28 (7) (1994) 1389–1393.
- [42] M.A. Oturan, J. Peïroten, P. Chartrin, A.J. Acher, Complete destruction of *p*-nitrophenol in aqueous medium by electro-Fenton method, *Environ. Sci. Technol.* 34 (16) (2000) 3474–3479.
- [43] A. Kesraoui-Abdessalem, N. Oturan, N. Bellakhal, M. Dachraoui, M.A. Oturan, Experimental design methodology applied to electro-Fenton treatment for degradation of herbicide chlortoluron, *Appl. Catal. B: Environ.* 78 (3/4) (2008) 334–341.
- [44] K. Vel Leitner, M. Doré, Mécanisme d'action des radicaux OH sur les acides glycolique, glyoxylique, acétique et oxalique en solution aqueuse: Incidence sur la consommation de peroxyde d'hydrogène dans les systèmes H<sub>2</sub>O<sub>2</sub>/UV et O<sub>3</sub>/H<sub>2</sub>O<sub>2</sub>, *Water Res.* 31 (6) (1997) 1383–1397.
- [45] D. Gandini, E. Mahé, P.A. Michaud, W. Haenni, A. Perret, Ch. Comninellis, Oxidation of carboxylic acids at boron-doped diamond electrodes for wastewater treatment, *J. Appl. Electrochem.* 30 (12) (2000) 1345–1350.
- [46] E. Guivarch, S. Trevin, C. Lahitte, M.A. Oturan, Degradation of azo dyes in water by electro-Fenton process, *Environ. Chem. Lett.* 1 (1) (2003) 38–44.